A grazing incidence diffraction setup for Langmuir trough experiments at the high-resolution diffraction beamline P08 at PETRA III

Journal of Physics: Conference Series **2380** (2022) 012047 doi:10.1088/1742-6596/2380/1/012047

A grazing incidence diffraction setup for Langmuir trough experiments at the high-resolution diffraction beamline P08 at PETRA III

Chen Shen, René Kirchhof, Florian Bertram

Deutsches Elektronen-Synchrotron DESY, Notkestrasse 85, Hamburg 22607, Germany

Corresponding authors' Email: chen.shen@desy.de, florian.bertram@desy.de

Abstract. The Langmuir Grazing Incidence Diffraction setup at the high-resolution diffraction beamline P08 of PETRA III is a dedicated setup for grazing incidence X-ray scattering measurements on Langmuir troughs. The instrument is optimized for low background grazing incidence X-ray diffraction measurements at vapour-water interfaces, while offering rapid layer structure assessment by grazing incidence X-ray off-specular scattering, and interfacial element analysis by total reflection X-ray fluorescence spectroscopy. Its control system is intuitive and standardized to provide easy access for non-expert users, and permits automated operation except for sample exchange.

1. Introduction

Interfaces between hydrophobic and hydrophilic media are abundant and important structures in nature, and are exploited for pharmaceutical applications, e.g. lipid nanoparticles for drug delivery [1], and nanotechnology [2]. Biomembranes, as one example, host essential life activities by serving as binding sites during signal transduction, and as host matrices for proteins while regulating their functions [3, 4]. Langmuir films at vapour-water interfaces are a typical model system for such studies with defined and adjustable thermodynamic conditions (composition, temperature, packing area and lateral pressure, etc.) [5]. Their structures can be obtained at near atomic resolution by surface sensitive X-ray scattering techniques [6]. In response to the increasing demand towards this application, we constructed a dedicated setup for Langmuir trough experiments at the high-resolution diffraction beamline P08 of PETRA III (DESY, Hamburg) [7]. The Langmuir Grazing Incidence Diffraction (Langmuir GID) setup is optimized for grazing incidence X-ray diffraction (GIXRD) with low background [8] to resolve lateral crystallographic order at vapour-water interface. Its layer structure can be assessed as rapidly as 10 s with grazing incidence X-ray off-specular scattering (GIXOS) [9], while total reflection X-ray fluorescence spectroscopy (TRXRF) provides information on the interfacial element accumulation [10]. The design of the control systems and data reduction aims at standardized and automated measurements.

2. Experiment setup

2.1. Default settings

The setup uses a customized Langmuir trough (modified Microtrough G4, Kibron Inc., Finland). By default the film area is controlled by one movable barrier (figure 1a). Optionally, a second movable

barrier can be installed to perform symmetric compression from two sides towards the trough center. Two Teflon trough plates are available: 600 mm × 155 mm (500 mL) with 1:8 compression ratio, and 350 mm × 155 mm (280 mL) with 1:4 compression ratio. The subphase temperature within the range between 5 and 40°C is controlled by a water circulation under the trough plate.

The trough is hosted on a translational stage in a helium-filled housing to reduce the background scattering from the vapour superphase (figure 1). The quarter arc Kapton exit window permits diffraction measurement up to a horizontal scattering angle $2\theta_h$ of 60°. Background scattering is further reduced by a guard pinhole (300 µm (v) × 1500 µm (h)) after the entrance Kapton window, and an 800 µm wide Tungsten strip before the exit window that catches the strong scattering on the specular plane [11]. A ground glass block is placed at the X-ray measurement area underneath the water to reduce the water depth below 1 mm, in order to damp long wavelength, low frequency surface vibrations [12].

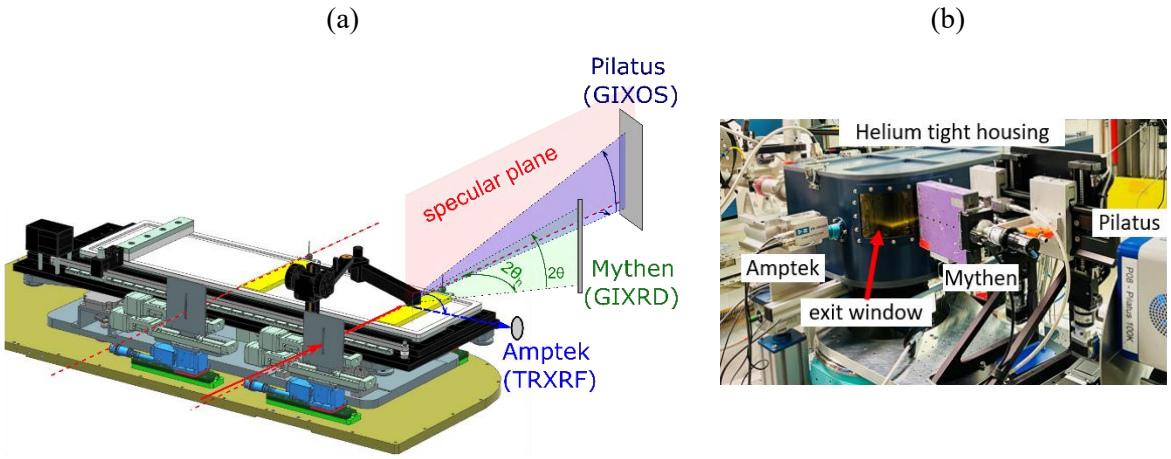

Figure 1. Sketch of the Langmuir trough on the translational stage of the housing (a) and the setup in operation (b), both under the default single barrier mode. The two areas in yellow are the 40 mm wide X-ray measurement area under the single and the double barrier mode (2nd barrier not shown). The red dashed lines depict the incident beam direction for both modes, through the pinhole and the beamstop. The solid red line shows the incident beam under the default mode. The GIXRD and GIXOS scattering planes and the TRXRF scattering direction are depicted in green, purple and blue, respectively. Their detectors are depicted in grey.

The setup is operated at a fixed incident angle that is 85% of the critical angle of the vapour-water interface, typically at 0.07° with 15 keV beam energy, with a flux of 6 ~ 10×10^{10} ph/s. It is achieved by deflecting the primary beam downwards by a quartz mirror. The default GIXRD detector module consists of a 1-dimentional position sensitive detector (Mythen2 1K, Dectris AG, Switzerland) that is vertically mounted at sample-detector distance of ~ 350 mm, and a Soller collimator (JJ X-ray A/S, Denmark) with 0.08° angular resolution (FWHM) in front of the detector [6] (figure 1). Each exposure covers a vertical scattering angle 2θ up to ~ 8° ($Q_z \in$[-0.05, 1.35 Å^{-1}]) while the full diffractogram I($2\theta_h$, 2θ) is acquired through a $2\theta_h$-scan of the Soller-Mythen module around the stage center. TRXRF data is recorded by an energy dispersive detector (Amptek X-123SDD, AMETEK Inc., USA) mounted into the housing at 3° from horizon, and 90° with respect to the beam direction, to minimize Compton and elastic scattering background [13]. The beam size for both TRXRF and default GIXRD is 70 µm (v) × 1000 µm (h). For GIXOS, a 250 µm wide vertical slit is mounted after the trough to defines the off specular scattering angle to Q_{xy} = 0.04 Å^{-1} [9]. A position sensitive detector (Pilatus 100k, Dectris AG, Switzerland) at 700 mm from the trough measures GIXOS intensity profile I(Q_z) up to 0.9 Å^{-1}, by 10 s ~ 120 s exposure. The horizontal beam size for GIXOS is 250 µm.

2.2. Optional settings

Optionally, grazing incidence small angle scattering (GISAXS) is performed by solely using the beamstop without the post-sample slit, such that a Q_{xy}-range from 0.01 and 0.3 $Å^{-1}$ is covered in one exposure by the GIXOS area detector.

The default GIXRD can be replaced by the pinhole camera GIXRD setup [14], to shorten the acquisition time to 20 s~120 s with a similar statistics, but on the cost of bearing an elevated and inhomogeneous background. The detector module consists of a 250 μm wide vertical slit at ~160 mm from the rotation center, the Pilatus 100k detector at ~500 mm distance, and a flight tube in between. Through the slit, different positions on the long X-ray footprint are projected onto different (horizontal) positions on the detector simultaneously, which corresponds to different horizontal scattering angles. One exposure covers a Q_{xy}-range of 0.6 $Å^{-1}$ (e.g. 1.1 ~ 1.7 $Å^{-1}$), and up to 1.0 $Å^{-1}$ in Q_z. The standard 250 μm slit gap, at 340 mm from the detector, provides a comparable angular resolution to the default GIXRD option, while higher count rate or better resolution can be achieved by choosing wider or narrower slit gap, respectively [14]. An unfocused beam of 120 μm (v) × 1000 μm (h) is used to provide a 100 mm long footprint with a homogenous illumination. The geometry and the conversion between the detector pixel indices and the scattering angle must be calibrated prior to the operation. We calibrate the exact distance between the detector and the rotation center by detector rotation. Thereafter, the distance between the slit and the detector is calibrated by the diffractogram from a silicon wafer coated with a ~300 nm polystyrene layer with embedded lanthanum hexaboride (LaB_6) powder (10 μm, Sigma-Aldrich Chemie GmbH, Germany) at the same incidence. An alternative calibration is using the integrated diffractogram from a LaB_6 capillary while it is moving along the beam between ±30 mm from the pivot point. More details on the pinhole geometry can be found in the work of Fontaine, et. al. [14].

In addition, the Langmuir trough can be operated under double barrier symmetric compression mode (figure 1). This is particularly suitable for experiments with rigid films where the Wilhelmy plate must be at the center of the compression to obtain valid tension values. The angular range for GIXRD is restricted to 30°, and TRXRF is currently not offered.

2.3. Experimental control and data reduction

The control of the X-ray measurements and the trough operation are fully integrated into the standard Sardana / SPOCK system of PETRA III [15]. The measurements are standardized and made intuitive to enable the scientists outside of the scattering community, in particular the first-time users, to perform useful measurements. Users typically compile blocks of commands to let the instrument automatically perform GIXOS / TRXRF / GIXRD measurements sequentially at various pressure / area settings and various temperature points.

Data reduction tools are available both online and offline to process and rebin GIXRD data into $I(Q_{xy}, Q_z)$ with orthogonal Q-space with a graphical user interface, and to process GIXOS and TRXRF data into $I(Q_z)$ and energy scale, respectively.

3. Example results

We present data from 1,2-dipalmitoyl-sn-glycero-3-phosphotidylcholine (DPPC) monolayer on water subphase as an example. Figure 2 shows two cycles of its Langmuir compression / expansion isotherm at 22°C, and the compression until the leakage of the trough at ~ 55 mN/m. The overlapping isotherms demonstrate the tightness and the reliability of the trough up to high surface pressure.

Data obtained by the standard GIXRD / TRXRF / GIXOS measurements is compiled into figure 3, together the optional pinhole-camera GIXRD data and GISAXS data, all collected at a surface pressure of 35 mN/m. The diffractogram measured by the default Soller-Mythen scan with 5 s exposure per $2\theta_h$ position and a $2\theta_h$-step size of 0.025° is completed in about 20 min (figure 3a). The maximum signal, found at the DPPC $(1\bar{1})$ Bragg rod [16] in the channel facing the Yoneda peak, is ~ 230 counts, while the water scattering contributes to a flat background signal of ~ 15 counts. Statistics are typically enhanced by binning the counts of every five Mythen channels. The complementary TRXRF spectra (figure 3b, 180 s exposure) show the K_α emission of phosphorus, located in the DPPC headgroup, at

2 keV. The emission at 3 keV, and between 8 keV and 13 keV, originates from the remaining Argon background and chamber background, respectively. These signals can be neglected since typical intensity values of adsorbed ions measured at this setup are at least 10 times stronger [10]. Its scattering length density (SLD) profile was obtained from the fitting of the GIXOS scattering pattern from a 120 s exposure [9] (figure 3c-d). Figure 3e shows the full GISAXS pattern of a DPPC monolayer (35 mN/m, 22°C), where the monolayer form factor is visible up to the third maximum ($2\theta \sim 5°$, $Q_z \sim 0.7$ Å^{-1}). The region close to the specular plane is blocked by the beamstop.

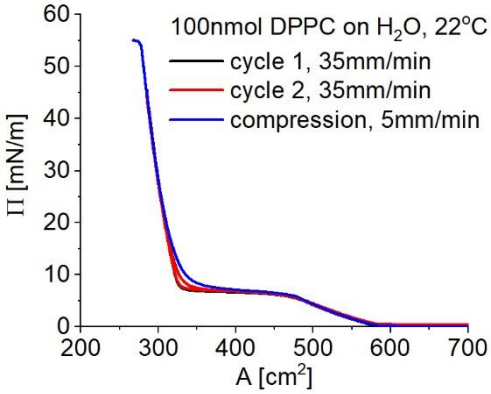

Figure 2. Langmuir isotherm cycles from a DPPC monolayer at water surface at 22°C.

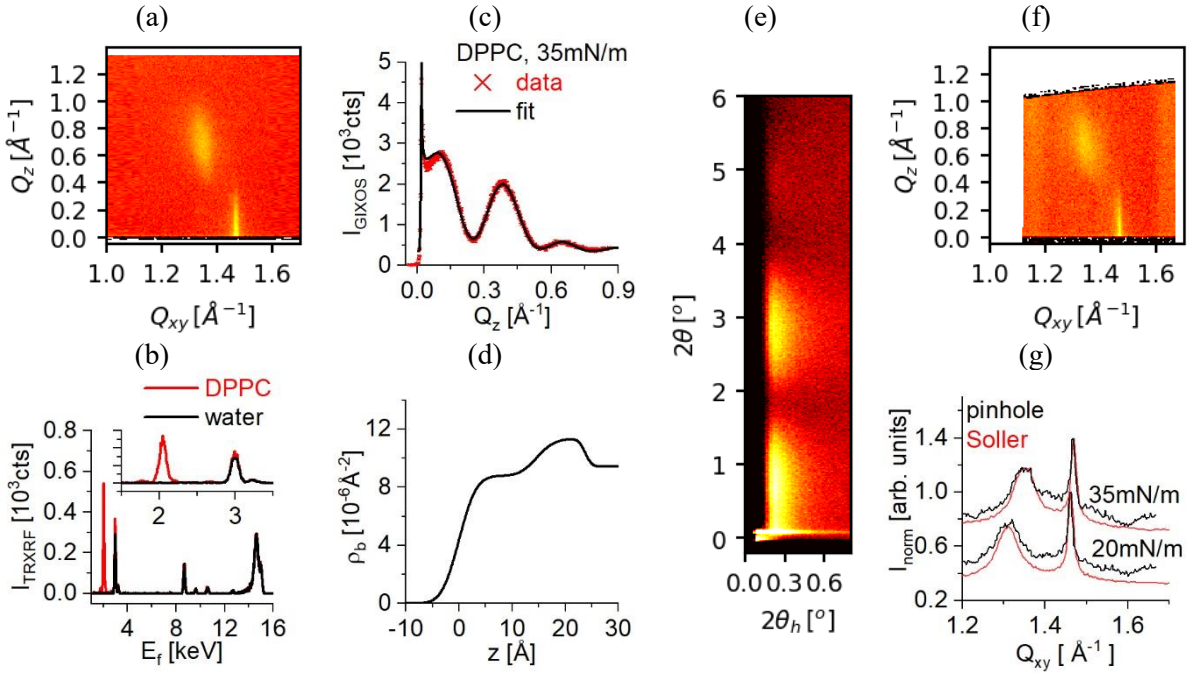

Figure 3. Data of DPPC monolayers at 35 mN/m at pure water surface at 22°C as an example. (a-c) GIXRD / TRXRF / GIXOS dataset obtained from the default setup settings. (d) SLD profile obtained from the fitting of GIXOS data. The depth origin z = 0 is defined at the air-tail interface. (e) GISAXS data. (f) Raw GIXRD data obtained from the pinhole camera mode. (g) Corrected pinhole-camera diffractograms, comparing to the GIXRD data from the Soller-Mythen mode. Data are integrated over Q_z, and data at two pressures are offset by 0.4.

The diffractogram obtained by a single shot exposure from the pinhole camera GIXRD mode is shown in figure 3f. Its statistics and Q_{xy} resolution are same as the one obtained from a 20 min scan under the default mode (figure 3a) using the Soller collimator. The diffractogram shows abnormally high intensity at the high and low Q_{xy}-edges of the field of view. This is due to the fact that each $2\theta_h$-position of the diffractogram corresponds to the diffraction from one particular position on the long footprint [14]. Consequently, the vertical beam profile, that results an uneven illumination along the footprint, is encoded into the diffractogram. The effect can be corrected by normalizing the diffractogram by water data under the same incident beam setting, as shown by the data from DPPC monolayers at 35mN/m and 20mN/m (figure 3g). Their Q_z-integrated diffractograms $I(Q_{xy})$ after the correction have an almost flat background on the two edges as the diffractogram from Soller-Mythen setting does.

4. Conclusion and outlook

This Langmuir GID setup at the high-resolution diffraction beamline P08 of PETRA III synchrotron provides low background, high quality diffraction data from Langmuir monolayers at vapour-water interfaces, that is complemented by rapid measurements of the layer structure and interfacial XRF emission. The standardized, intuitive and semi-automated experimental control eases its access for non-expert users. Moreover, an automated subphase exchange and injection pump system is expected to be integrated into the system by the autumn of 2022. This will provide a broader application of this setup, e.g. for kinetic studies on drug and peptides adsorption to biological membranes.

References

[1] Hou X, Zaks T, Langer R and Dong Y 2021 Lipid nanoparticles for mRNA delivery *Nature Reviews Materials*
[2] Boles M A, Engel M and Talapin D V 2016 Self-assembly of colloidal nanocrystals: from intricate structures to functional materials *Chem Rev* **116** 11220-89
[3] van Meer G, Voelker D R and Feigenson G W 2008 Membrane lipids: where they are and how they behave *Nature Reviews Molecular Cell Biology* **9** 112-24
[4] Casares D, Escriba P V and Rossello C A 2019 Membrane lipid composition: effect on membrane and organelle structure, function and compartmentalization and therapeutic avenues *International journal of molecular sciences* **20**
[5] Stefaniu C, Brezesinski G and Mohwald H 2014 Langmuir monolayers as models to study processes at membrane surfaces *Advances in colloid and interface science* **208** 197-213
[6] Als-Nielsen J and Kjær K 1989 X-ray reflectivity and diffraction studies of liquid surfaces and surfactant monolayers *Nato Adv Sci I B-Phy* **211** 113-38
[7] Seeck O H, Deiter C, Pflaum K, Bertram F, Beerlink A, Franz H, Horbach J, Schulte-Schrepping H, Murphy B M, Greve M and Magnussen O 2012 The high-resolution diffraction beamline P08 at PETRA III *J Synchrotron Radiat* **19** 30-8
[8] Pignat J, Daillant J, Leiserowitz L and Perrot F 2006 Grazing incidence X-ray diffraction on Langmuir films: Toward atomic resolution *J. Phys. Chem. B* **110** 22178-84
[9] Dai Y, Lin B, Meron M, Kim K, Leahy B and Shpyrko O G 2011 A comparative study of Langmuir surfactant films: Grazing incidence x-ray off-specular scattering vs. x-ray specular reflectivity *Journal of Applied Physics* **110** 102213
[10] Brezesinski G and Schneck E 2019 Investigating ions at amphiphilic monolayers with X-ray fluorescence *Langmuir* **35** 8531-42
[11] Pohlmann T, Hoppe M, Thien J, Dey A B, Alexander A, Ruwisch K, Gutowski O, Röh J, Gloskovskii A, Schlueter C, Küpper K, Wollschläger J and Bertram F 2022 Time-resolved x-ray diffraction and photoelectron spectroscopy investigation of the reactive molecular beam epitaxy of Fe_3O_4 ultrathin films *Phys. Rev. B* **105** 045412

[12] Als-Nielsen J, Jacquemain D, Kjaer K, Leveiller F, Lahav M and Leiserowitz L 1994 Principles and applications of grazing-incidence x-ray and neutron-scattering from ordered molecular monolayers at the air-water-interface *Phys. Rep.-Rev. Sec. Phys. Lett.* **246** 252-313
[13] Das G, Tiwari M K, Singh A K and Ghosh H 2014 Effect of synchrotron polarization on grazing incidence X-ray fluorescence analysis *Journal of Analytical Atomic Spectrometry* **29** 2405-13
[14] Fontaine P, Goldmann M, Bordessoule M and Jucha A 2004 Fast and adjustable-resolution grazing-incidence x-ray liquid surface diffraction *Rev. Sci. Instrum.* **75** 3097-106
[15] Coutinho T, Cuní G, Fernandez-Carreiras D, Klora J, Pascual-Izarra C, Reszela Z, Suñé R, Barcelona S, Homs E, Taurel V and Rey E 2021 Sardana, the software for building scadas in scientific environments
[16] Brezesinski G, Dietrich A, Struth B, Bohm C, Bouwman W G, Kjaer K and Mohwald H 1995 Influence of ether linkages on the structure of double-chain phospholipid monolayers *Chem Phys Lipids* **76** 145-57

Acknowledgement
We acknowledge DESY (Hamburg, Germany), a member of the Helmholtz Association HGF, for the provision of experimental facilities. This research was carried out at PETRA III. We thank Dr. B. Ocko (NSLS-II) for the valuable discussion, Prof. G. Brezesinski (Martin Luther University Halle-Wittenberg) and Mr. O. Gutowski (DESY) for the improvement of TRXRF measurements, all users of this setup for their suggestion in improving the experimental control systems, and Dr. M. T. Nunez Pardo de Vera (DESY) for integrating the trough control into the experimental control at PETRA III. We thank Mr. C. Johans and Dr. P. Soumalainen (Kibron Inc.) for their efforts in customizing the Langmuir trough and providing the protocol for remote trough control.